Substrate Integrated Waveguide (SIW) Techniques: The State-of-the-Art Developments and Future Trends

DJERAFI Tarek[1] and WU Ke[2]

(1. INRS-Energy, Materials, and Telecommunication Montreal QC Canada H5A 1K6;

2. Poly-Grames Research Center, Ecole Polytechnique of University of Mntreal, Center for Radiofrequency Electronics Research of Quebec Montreal QC Canada H3C 3A7)

Abstract The state-of-the-art developments of substrate integrated waveguide (SIW) techniques is overviewed. Various SIW-based passive and active components reported so far have demonstrated that they can be effectively integrated in the form of low-cost system-on-substrate (SoS), which provides complete packaged system solutions. Different innovative SIW beam-forming techniques are discussed. Future developments are forecasted, which suggest the expansion of substrate integrated circuits (SICs) into 3-D geometry and mixed integrations of dissimilar waveguides within the same substrate building blocks. Other SIW-related trends are also described, including non-linear and active waveguide developments as well as CMOS-based waveguide synthesis for millimeter-wave and THz applications.

Key words millimeter-waves; substrate integrated circuits (SICs); substrate integrated waveguide (SIW); system-on-substrate (SoS); terahertz

基片集成波导技术：最新的发展及未来的展望

塔利克·吉纳菲[1]，吴 柯[2]

(1. 国家科学研究中心能源-材料与通信分部 加拿大 魁北克 蒙特利尔 H5A 1K6;

2. Poly-Grames研究中心 蒙特利尔大学工学院 魁北克射频电子研究中心 加拿大 魁北克 蒙特利尔 H3C 3A7)

【摘要】回顾了基片集成波导技术(SIW)最新的发展动态。到目前为止，所报道的各种各样基于基片集成波导技术的无源和有源元器件已经证明，它们能够被有效地集成为低成本基片片载系统(SoS)，为封装系统提供了完整的解决方案。讨论了不同的创新型基片集成波导的波束形成技术，展望了未来的发展方向，提出了将基片集成电路扩展到三维空间以及在相同的基片构建模块上将不同的波导结构进行混合集成的思想，描述了用于毫米波和太赫兹应用的基片集成波导技术其它的发展趋势，这包括非线性和有源波导的开发以及基于CMOS技术的波导合成。

关 键 词 毫米波; 基片集成电路(SICs); 基片集成波导(SIW); 基片片载系统(SoS); 太赫兹

中图分类号 TN015 文献标志码 A doi:10.3969/j.issn.1001-0548.2013.02.002

With an ever-growing number of possible applications in the area of broadband wireless communications, high-speed machine-to-machine (M2M) interconnectivity, collision avoidance radar, imaging systems and other countless wireless sensors and networks, the development of low-cost and innovative transmitter and receiver front-ends in the millimeter-wave range has stimulated an unprecedented enthusiasm in both academia and industry[1-3]. Millimeter-wave techniques are well known to hold the promise in the above mentioned applications thanks to diverse advantages and unique features, just to name a few of them: the availability of large bandwidths that increase the spatial resolution for imaging or localization and also enhance data transmission rates for communication; the atmospheric attenuation and scattering in connection with various molecular effects(rain and fog, e.g.) that are useful for

Received date： 2013 – 02 – 15

收稿日期： 2013 – 02 – 15

Foundation item: Supported by NSERC of Canada and FQRNT of Quebec.

基金项目：加拿大国家科学和技术研究委员会(NSERC)资助; 魁北克自然和技术研究资金会(FQRNT)资助

Biography：DJERAFI Tarek was born in 1975, and his research interests include passive and active components, antenna arrays, beamforming networks.

作者简介：塔利克·吉纳菲 (1975 –)，男，博士后，主要从事无源和有源电路、天线阵列的波束形成网络方面的研究.

facilitating frequency re-use and planning; the reduction of wavelength decreasing system size and increasing antenna array gain. Generally speaking, the requirements for commercial millimeter systems are not limited to performances but to size and cost, which have been the fundamental hurdles for the successful deployment of a millimeter-wave device or system on the market.

Since the transmission line technology is instrumental for developing high-frequency electromagnetic hardware, the choice of an appropriate waveguide or line structure is critical for millimeter-wave developments and applications. The adopted transmission lines should allow high-density integration and mass-producible scheme at low cost. Rectangular waveguides have widely been used in the development of microwave and millimetre-wave components and systems with their salient features such as low insertion loss, high quality factor (Q-factor), high power capability, etc. However, they are also characterized by their bulky size, stringent manufacturing precision, and non-planar geometry. Therefore, it is impossible to design and develop microwave and millimetre-wave integrated circuits with this technological platform. Benefiting from the properties of low profile, easy fabrication, and low cost, microstrip-like circuits including coplanar waveguides (CPW) and strip lines are presently the principal choice of integration for the development of microwave and millimetre wave circuits. Unfortunately, such printed circuits suffer from significant losses and packaging problems. In fact, the performances of microstrip-like circuits are fundamentally limited by physical properties such as the field or current singularities at the stripline[4].

SIW structure preserves most of the advantages associated with conventional metallic waveguides, namely high Q-factor (low loss) and high power-handling capability with self-consistent electromagnetic shielding. The most significant advantage of SIW technology is its power of enabling a possible complete integration of all the components on the same substrate, including passive components, active elements, and even antenna[5-9]. SIW techniques can be used to solve a series of headache problems, which renders its huge popularity in the community today[10]. A remarkable problem arising at high frequency is the appearance (trapping) of surface waves which generally decrease the antenna efficiency. The SIW can effectively control this phenomenon. Since SIW components are covered by conducting surfaces on both sides of the substrate, they exhibit the merits of low insertion loss, extremely low (completely negligible) radiation/leakage loss, and insensitive to outer interference. The SIW technology has already spanned a rapid development over more than one decade. This development allows the demonstration and application of innovative passive and active circuits, antennas, and systems at microwave and millimeter-wave circuits covering a very broad frequency range from sub-gegahertz to sub-terahertz. In addition, the SIW technique can be combined with other SICs platforms to create multi-format and multi-function devices and systems[9].

This paper begins with a brief description of the SIW concept. Subsequently, the SIW techniques are examined for various RF, microwave and millimeter-wave applications, which highlight the merits of different SIW components. Examples of novel devices and design techniques are presented, and SIW-based couplers, filters, phase shifters, and others are reviewed and discussed. A number of SIW-related applications are shown. In particular, this paper looks into the integration of active devices based on SIW schemes, which exploit some of the unique SIW characteristics in the design of oscillators, mixers and amplifiers. And also, SIW-based antennas and beam forming networks in connection with these antennas are discussed. Finally, the future trends of SIW techniques and their interesting aspects are presented.

1 SIW Techniques and Design Basics

SIW is a rectangular waveguide-like structure in an integrated planar form, which can be synthesized and fabricated by using two rows of conducting cylinders or vias or slots embedded in a dielectric substrate that is electrically sandwiched by two parallel metal plates as illustrated in Fig. 1. In this way, the

non-planar rectangular waveguide can be made in planar form. As a general observation, SIW components can be manufactured with any processing techniques such as printed circuit board (PCB) process, low temperature co-fired ceramic (LTCC) technique and photo-imageable process, to name a few. The operating frequency range is delimited by the monomode propagation of quasi-TE_{10} wave as its cut-off frequency is only related to equivalent width a_{eq} of the synthesized waveguide as long as the substrate thickness or waveguide height is smaller than this width. This equivalent width will be discussed in the following section.

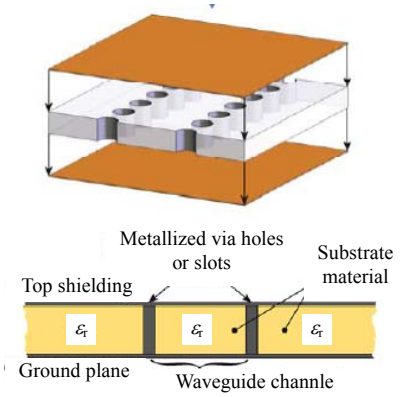

Fig. 1　The topology of a typical single-layered SIW

1.1　Via configurations

Round metalized via holes are used to create the electric side walls or fences of SIW through two parallel via arrays. The discontinued current flow along the via- or slot-synthesized metalized side walls does not allow the propagation of TM modes. In addition, the large width-to-height ratio of SIW supports the propagation of TEm0 modes. The SIW can be modeled by a conventional rectangular waveguide (RW) through the equivalent width a_{eq}. This parameter is calculated such that the resulting dielectric-filled rectangular waveguide has the same cut-off frequency of the fundamental TE_{10} mode as its corresponding SIW structure. This determines the propagation characteristics of TE_{10} mode. Physical parameters of via-holes d and p are set to minimize the radiation (or leakage) loss as well as the return loss[11]. The equivalent rectangular waveguide width can be approximated according to the geometrical parameters illustrated in Fig. 2 as follows:

$$a_{eq} = a_{SIW} - \frac{d^2}{0.95p} \tag{1}$$

Processing techniques such as laser micromachining perforation or wet/dry etching can also be used to fabricate and define the two via arrays. Since these techniques are amenable to arbitrarily shaped perforations, the limitation to circular vias is no longer mandatory. Rectangular slot trenches were found to be advantageous for lower leakage and better definition of the SIW side walls. This is important for some details such as those iris and window coupling geometries found in the filter design. Rounded corners increase the overall mechanical stability, allowing for better metallization, which often cannot be avoided in the fabrication process due to the finite diameter of laser beams. Fig. 2 shows two different slot trench configurations: (b) shorter slots for SIW operation below its first stop band and (c) longer slots for SIW operation between the first and second stop bands. Note that the SIW structure is a periodic geometry, which is subject to the guided-wave phenomena of all periodic waveguides such as bandgap (stop band) effects. Stop bands, caused by the distributed Bragg reflection, occur around frequencies where the periodic spacing p is equal to a multiple of half a guided wavelength[12].

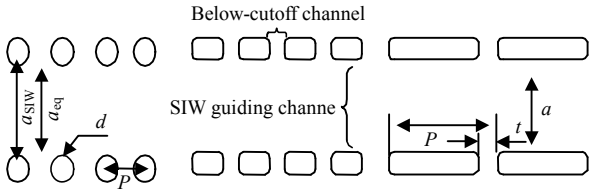

a. Cylindrical via arrays　b. short slot trenches　c. long slot trenches

Fig. 2　Metalized via and slot arrays for creating equivalent metallic fences or walls configurations

1.2　Substrate materials

Low-loss material is the foundation for developing high-performance integrated circuits and systems. This becomes more critical for power budget as frequency increases to the millimeter-wave ranges and beyond. This is because it is relatively difficult to amplify over those ranges. Thermal effect, dielectric non-uniformity and metallic surface roughness may have to be taken into account for better and accurate design. This is especially critical for antenna developments. The SIW can theoretically be

constructed with any available substrate. The most used ones are Rogers RT/duroid®5880 glass microfiber reinforced PTFE composite and RT/duroid®6002 for conventional PCB processing, which are easily sheared with laser and machined to the required shape. The holes can easily be drilled mechanically into these machinable materials compared to ceramics which can only be processed by the laser perforation. All these materials have an excellent dimensional stability. Of course, a good thermal stability of the material of choice should also be considered in the design.

1.3 Loss considerations

The energy in transmission is lost or dissipated through different mechanisms including dielectric losses, conductor losses, and radiation losses. Since the inner part of SIW is filled with a dielectric material, an adequate choice of dielectric material and conductor thickness can reduce the contribution of the first two loss mechanisms.

Radiation or leakage leads to two consequences, namely additional signal losses and undesired interferences. In order to ensure that the synthesized waveguide section becomes radiationless or free from leakage loss, parametric effects of p and d were studied on those issues in [11]. To simplify the analysis, dielectric and conductor losses are not considered, the loss solely comes from radiation. It is found that the following requirements can be put forward to minimize return and leakage losses, that is, the diameter of hole should satisfy some geometric constraints:

$$d < \frac{\lambda_g}{5}, p \leqslant 2d \tag{2}$$

At millimeter and sub-millimeter frequencies, planar circuits usually suffer from radiation originating at bends and discontinuities. 90 degree SIW and microstrip bend losses were analyzed in [13] in the 77 GHz band. A 100 ohm circular microstrip line bend is considered with a radius equivalent to the SIW line radius of 2 mm and a substrate of 10 mil with ε_r=2.95. The total losses are the linear addition of radiation losses, conductor losses and dielectric losses. The two bends are shown in Fig. 3 with electric field plots. Fig. 4 shows simulation results of the defined SIW and microstrip bends. In this case, the loss at the SIW bend is about 0.12 dB compared to 0.36 dB in connection with the microstrip bend, and in fact negligible radiation losses are found from the SIW structure when the conditions (2) are respected. The major part of losses in microstrip is related to radiation.

Fig. 3 E-field distribution along SIW and microstrip bends

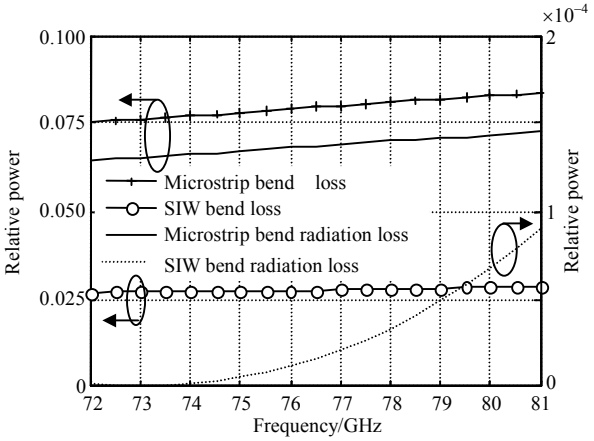

Fig. 4 Loss in SIW and microstrip bends

1.4 Power handling

Generally, the average power handling capacity of an SIW structure is primarily determined by its substrate materials and its geometric topology. This is especially related to its structural heat endurance and dissipation ability as well as the electric breakdown voltage of the materials, which is in turn dependent on the thickness of substrate and material properties. In practice, the SIW components often involve the use of microstrip lines and other printed lines, which, in fact, determine the maximum power handling capability instead of the SIW-based circuits. The power handling capability depends on the nature of those SIW circuits. Usually, well-matched traveling-wave circuits can handle much more power than those counterparts with mismatch conditions and resonances. In the case of filter designs, the SIW cavity resonators are fundamentally responsible for power handling capability in addition to the microstrip-to-SIW transitions[14-15].

Using the popular Rogers substrate RG5880 with: thickness of 0.508 mm, d=0.4 mm, p= 0.8 mm and

a_{eq}= 15 mm, up to 450 W at 10 GHz for well-matched and non-resonant SIW interconnects and transmission lines can be expected[16]. The SIW techniques are found to provide a very attractive and promising power handling capability for nearly all of the established and planned wireless systems for commercial applications.

In the following sections, a few selected passive and active SIW-based components and circuits are presented and discussed without getting into the extensive diversity of the current SIW developments. So far, so many technical publications and reports have been found in various journals and conferences on various SIW components, devices, circuits and systems. The detail of such an explosive progress cannot be reviewed in the limited space of the present article.

2 Passive SIW Components and Circuits

2.1 Couplers

Directional couplers have widely been used in RF, microwave, and millimeter applications such as in precision measurement systems (weak coupling), six-port transceivers and mixers (3 dB coupling), beam forming, and other antenna feeding networks (various coupling ratio).

As the first example, the well-known Riblet short-slot coupler consists of two waveguides with coinciding H-planes. The common wall is removed over a defined length in order to obtain the desired coupling. The output signals of the coupler are 90 degree out of phase. The geometry of the coupler is determined on the basis of a simple even/odd mode analysis where the even mode is related to the TE_{10} mode and the odd mode is related to the TE_{20} mode. A scheme of widely used Riblet short-slot directional coupler is shown in Fig. 5. One[17] and multiple steps[18] are used to prevent propagation of the undesired the TE_{30} mode. The matched H-plane impedance steps can be substituted by continuous line. The entire width of the common broadside wall of two adjacent SIWs may lead to a coupling value between 0 dB and 7 dB. For achieving a lower coupling factor, multiple apertures must be used with variable length[17,19]. The only parameters subject to optimization are the number of apertures and their lengths. In fact, those geometrical parameters define a non-uniform field-coupling distribution in the form of Taylor or Chebyshev functions. Fig. 6 shows the configuration of a typical directional coupler with three apertures. The cruciform H-plane coupler was proposed in SIW technology in [20] and improved in [21]. This coupler has the capability to achieve a wide range of coupling ratios while maintaining a very compact size since the coupling occurs in the crossing area of two simple SIW transmission lines as shown in Fig. 7. Furthermore, this perpendicular configuration is particularly adapted to Blass or Nolen beam-forming matrices. Two metallic posts (vias) are diagonally positioned in the crossing area to achieve a desired coupling. Another class of coupler enabled by the SIW technology is called quasi-optical coupler. This type of coupler is composed of four SIW branches, connected in the form of a cross with a mirror obstacle disposed diagonally in the junction region[22]. To create the needed effective permittivity variation, grating in the form of fringe planes running parallel to each other through the depth is added as shown in Fig. 8.

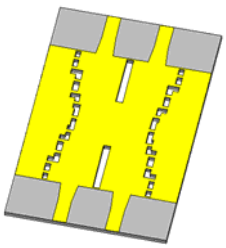

Fig. 5　Short slot coupler with impedance steps

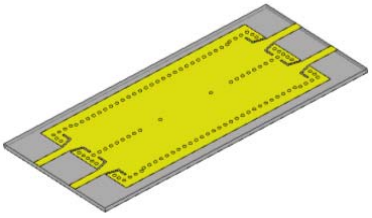

Fig. 6　Multi-aperture couple

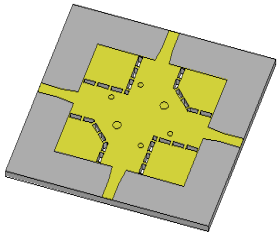

Fig. 7　Cruciform coupler

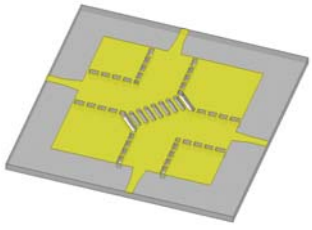

Fig. 8　Quasi- optical coupler

On the other hand, a class of H-plane hybrid rings

(rat-race type) has been designed on the SIW technique[23] and on a folded SIW scheme[24]. A dual band ring coupler has been reported in [25] where the left handed propagation is explored together with the half-mode SIW structure, yielding a compact design. However, limited frequency ratios can be achieved (~1: 1.6 typically). The coupler illustrated in Fig. 9 has an original structure based on two concentric rings in a double-layer ridged SIW topology with de-multiplexing scheme. A simple design methodology has been described and a C/K-band prototype with a 1:2.8 frequency ratio has been experimentally validated[26]. Different variations of SIW (half mode, folded and ridge) lead to additional advantages in terms of size, bandwidth and others.

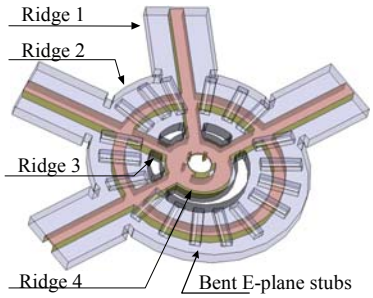

Fig. 9 Configuration of the ring (rat-race) hybrid loaded with stubs

The performance of this broadside-wall directional coupler is nearly identical to that of a narrow-side coupler with the same slot dimensions. In the design demonstrated in Fig. 10, two slots of the same dimension are cut on the common broadside-wall of two waveguides[27]. For the multi-aperture counterparts, the apertures are located adjacent to the boundary side-wall of waveguide, equidistant from the guide center-line, opposite from each other, and in a longitudinal position (circular apertures are used in [17]). Correction factors were introduced to take into account the frequency dependence of the circular aperture and the thickness of the wall where the apertures were drilled.

Table 1 summarizes the performances of different couplers as well as the total size. The choice of a coupler type depends on the required bandwidth, coupling ratio, and fabrication tolerance. Of course, the fabrication factor is also directly related to operating frequency. It is expected that millimeter-wave design and development could be more delicate with reference to the fabrication tolerance.

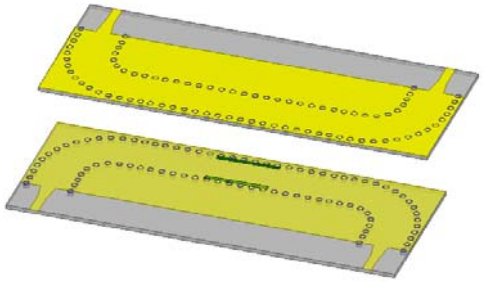

Fig. 10 Configuration of the E-plane coupler

Table 1 Comparison of various coupler performances

Coupler	Freq/ GHz	Bandwidth/ (%)	Coupling /dB	Isolation /dB
Riplet[18]	76.0	15.7	3.18±0.1	25.0
Two apertures[19]	25.5	11.0	4	12.5
Cruciform[21]	12.5	28.0	3.25±0.25	20.0
Quasi-optical[22]	24.0	20.0	3.4±0.5	20.0
Rat race[24]	26.0	12.7	4.3	20.0
E-plane[27]	28.0	20.0	3.5±0.5	18.0

2.2 Filters

SIW-based filter design has received particular attention due to the possibility of achieving a high quality-factor and also a better selectivity compared to classical planar filters. Probably, SIW bandpass filters have been the most popular and also the most studied SIW components in the literature.

The simplest form, which is also the earliest SIW filter, is the inductive post filters reported in [28]. A 3-pole Chebyshev filter bas been designed and manufactured and its design procedure (Fig. 11) was detailed in [28]. The most popular type is related to the use of post-wall iris techniques[29-30]. Fig. 12 illustrates the geometry of this filter. Different cavity shapes can be used such as circular and elliptic forms[31]. The introduction of extra cross-couplings provides a better control of transmission zero positions in order to achieve a better fitting of electrical response. The authors in [32] proposed a zigzag filter topology (Fig. 13), which includes additional controllable cross-couplings in order to realize a sharper response and a more flexible tuning of transmission zeros. Cross-coupled filters can be realized by introducing complementary split ring resonators (CSRRs) on the top metal plate. A novel bandpass filter was proposed and demonstrated in [33], which was implemented with a combination of CSRRs and SIW as shown in Fig. 14, the CSRRs provide a negative effective

permittivity in the vicinity of resonant frequencies and produce a sharp rejection stop band. To accomplish a negative coupling as shown in Fig. 15, TE201-mode response is used in the first cavity, which is also used to implement a cross-coupling with TE101 mode for generating additional transmission zeros (TZs) in the stopband of the filter[34]. Two additional TZs are introduced and the stopband performance is then improved. A compact SIW filter with defected ground structure (DGS) was proposed in [35]. The DGS is etched on the ground plane of SIW cavities, and it behaves as a resonator. Under such a condition, better frequency selectivity attributed to three transmission zeros is obtained, and two of them are located at the lower stop band.

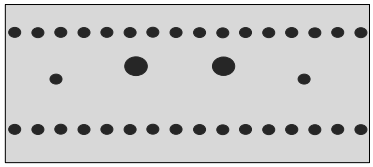

Fig. 11　Inductive post filter

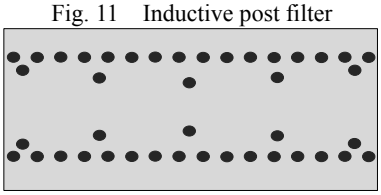

Fig. 12　Iris-coupled filter

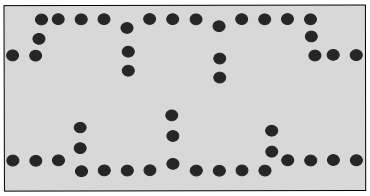

Fig. 13　Seven-pole filter in zigzag meandered topology

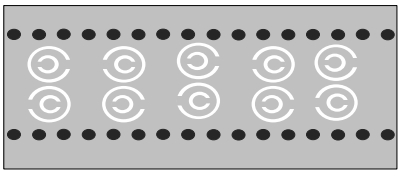

Fig. 14　Complementary Split Rings Resonators (CSRRs) filter

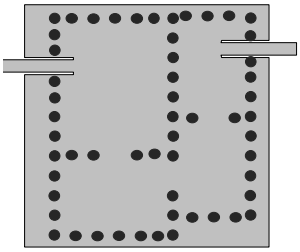

Fig. 15　Cross-coupled cavity filter.

A 7th order filter was designed in [36] at the center frequency of 34.5 GHz. Based on iris cavities assembled in the E-plane to reduce the size, the filter provides sharp frequency selectivity. To control the cavity coupling factor and the matching condition, four conducting vias are inserted in the main waveguide path, two on each side of the transversal cavity (Fig. 16). This leads to a beautiful Lego-style design.

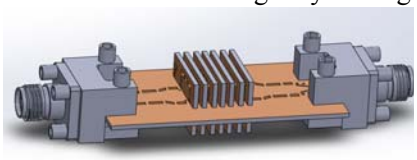

Fig. 16　Configurations of seven pole E-plane cavities filter[36]

A multilayer structure was proposed in [37], which can provide a more freedom and flexibility of coupling design in both horizontal and vertical directions for a more compact geometry. Coupling between cavities is mainly controlled by metallic via walls between adjacent cavities while the coupling between cavities in different layers is mainly managed by apertures etched on layer interfaces as shown in Fig. 17.

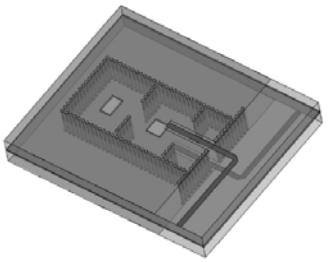

Fig. 17　Multilayer SIW filter (MSIW)[37]

Various filter performances are summarized in Table 2 and show a wide range of flexibility to generate a desired frequency response. A different number of poles have been design for each filter. Each filter design has its own advantages and shortcomings. An overview of the SIW filter with different constraints were presented in two different workshop sessions[14-15].

Table 2　comparison of various filter performances

filter	BW/(%) (f_0 GHz)	Pole/Zero	Il/dB	Size/(λ_g^2)
Inductive posts[28]	3.6 (28)	3 poles	1.1	0.75×2
Iris[30]	9 (10)	8 poles	4.0	0.75×10.8
Zigzag[32]	28 (7.5)	7 poles/ 3 zeros	1.2	1.5×1.2
CSSRs [33]	20 (7.25)	4 poles	1.5	///
Cross coupled[34]	3 (20)	2 poles/4 zeros	1.7	1.9×1.5
DGS[35]	9.2 (4.9)	4 poles	1.1	0.7×0.7
E-plane iris[36]	2.9 (34.5)	7 poles	2.9	1.2×2.2
MSIW[37]	3.75 (4)	4 zeros	0.6	0.79×1.55

2.3　Additional components

A series of SIW components other than couplers and filters are documented and reported in the

literature. The components which include phase shifter, power divider (T and Y) and bends in the two planes are also indispensable in building of front-end system. In the following, typical examples are presented.

The phase shift can be realized by means of unequal–length unequal–width transmission lines. The topology of such a phase shifter is shown in Fig. 18. A differential phase shift of 45+0.4° was achieved in [18], together with a reflection coefficient less than -20dB over a wide frequency range of interest (16%). An H-plane wideband SIW phase shifter structure was realized by stub loading in [38] to cover the V-band. It makes use of two transmission lines, namely a reference line and a line containing several stubs (two in this case). If the same signal is sent though the reference line and the line containing stubs, the two output signals are subject to a nearly flat phase difference over 16% of frequency band. In [39], the phase shift mechanism was studied on the basis of a synthesis of low dielectric slab in the middle of SIW using an array of air holes. A simple design technique is proposed, where unit cells are simply cascaded, which leads to the summation or accumulation of their phase shift. The number of holes, their diameter and their spacing can be adjusted in order to obtain a required phase shift, thus giving a very flexible structure. An experimental validation in the Ka band shows excellent results from 30 GHz～40 GHz.

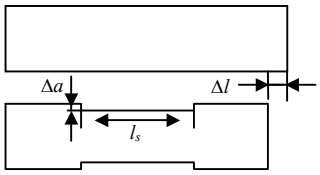

Fig. 18 H-plane SIW phase shifter

To prevent reflections at the unused port in coupler or six-port circuit, a load should be integrated. A resistive attenuator is added before the short circuit at the end of an isolated port. This attenuator is fabricated once the whole circuit is finished by etching the copper using a thin titanium sputtered film as illustrated in Fig. 19 for the six-port design case. A dielectric capping layer can then be added to prevent titanium oxidation and also to improve a long-term stability. The power divider and six-port circuit using this principle have been presented in [21], confirming that the added attenuator has no effect on the transmission coefficient or desired phase shifting.

Different Wilkinson power dividers/combiners were proposed and developed with various SIW techniques in [40-41]. In [40], SIW structure is used in constructing three branches while the half mode (HM) SIW technique is deployed in the design of the quarter-wave transformer. Reasonable results are shown for 17% bandwidth with 10 dB of isolation/ matching. A double-layered X-band Wilkinson power divider/combiner (Fig. 20) based on the SIW technique was proposed in [41], ensuring a good performance over 25% of bandwidth.

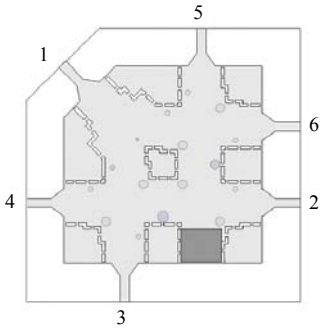

Fig. 19 Resistive termination in SIW six-port circuit

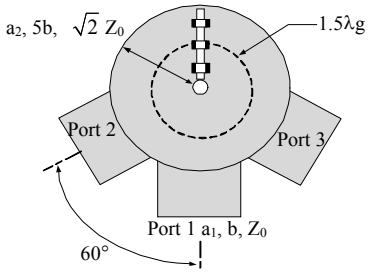

Fig. 20 Wilkinson power divider

The first publication about microwave ferrite devices using SIW technology such as circulators and isolators has been presented in [42]. For emerging high volume applications, efforts are focused on the integration of SIW circulators[43]. An 18% bandwidth at 22 GHz with an insertion loss better than 1.3 dB was obtained. The circuit illustrated in Fig. 21 is capable of handling a medium power level and can easily be integrated with other planar components.

A large number of applications require the integration of non-planar topologies or the extension of H-plane into E-plane (vertical integration) operations such as E-plane bend, T-junction and magic-T as shown in Fig. 22. These components were studied and

developed with success in [44]. For the H-to-E plane interconnection (E-plane bend), the measured results have shown a very good performance over 28% bandwidth around 35 GHz. A wideband T-junction power splitter with 180 degree phase shift between the outputs is then introduced, designed, and fabricated. The measured phase imbalance of the SIW T-junction is found less than ±4 degree from 32 GHz～38 GHz. Moreover, the three-dimensional (3-D) SIW magic-T is also studied and demonstrated, which features low cost, compact size, and high isolation. All of the four branches are in the same layer thanks to E-plane bends. The in-phase phase imbalance is ±2.5 degree and the out-of-phase phase imbalance is ±7.5 degree, respectively from 30 GHz～38 GHz.

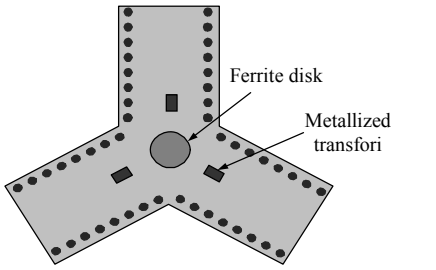

Fig. 21　SIW circulator

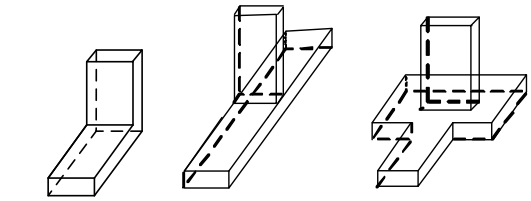

Fig. 22　E-plane structures

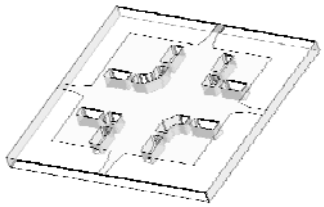

Fig. 23　3-D view of the SIW crossover coupler

SIW cross-over junctions are very useful for the development of high-performance and compact-sized Butler matrices. A junction proposed in [45] is composed of four rectangular waveguide branches or arms, connected in the form of a cross (Fig. 23). The reflecting obstacle in the junction region is avoided to produce a cross-over coupler. The 0 dB coupler is realized at 60 GHz frequency. Measurements on the realized prototypes show a 5% relative bandwidth with less than 0.2 dB coupling loss.

3　Active SIW Devices and Circuits

3.1　Tunable filters

Electrically and/or magnetically tunable filters are able to facilitate the architecture simplification of multiband and wideband wireless systems. Through a dynamical and fast reconfiguration of the operation frequency and bandwidth, the tunable techniques offer an unprecedented opportunity for developing multi-format and multi-function transceivers for cognitive and software-defined systems. Note that the tunable devices may not be classified into active circuits as amplifier and others but they are subject to design approach in connection with linearity and other parameters of active devices.

A very recent tunable SIW filter presented in [46] consists of a tunable evanescent-mode SIW cavity, and two tunable impedance matching networks. The evanescent-mode SIW cavity is loaded with a pair of tunable mushroom-type CSRRs. When the SIW cavity is tuned, its input impedance alters from low end to high end. The mismatch to the 50 ohm external ports compromises the transmission. A pair of tunable impedance matching networks is implemented right at ports of the SIW cavity, as depicted in Fig. 24. The whole module is based on an aluminiumoxide ceramic substrate with a Cu-doped Ba Sr TiO (BST) thick-film screen printed on the top.

The filter proposed in [47] for wireless systems is a basic two-polegeometry developed using packaged RF MEMS switches. It utilizes a two-layer structure to isolate the cavity filter from the required RF MEMS switch circuitry (mainly voltage drivers). Tuning elements, consisting of via-posts and RF MEMS switches, are placed at various locations within the cavity, as shown in Fig. 25. Metallic vias between the top and bottom metal layers are used to tune the resonance frequency of the cavity. To avoid shorting a tuning post to the cavity top wall (middle metal layer), square openings with edge in the cavity's top wall are placed around each tuning post. Since these openings are small compared to the dimension of the cavity, the

cavity fields remain relatively unaffected.

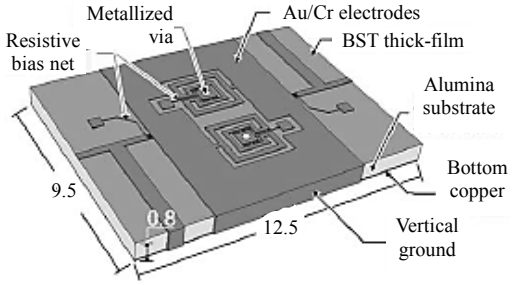

Fig. 24 The proposed tunable filter implemented with BST/ceramic substrate[46]

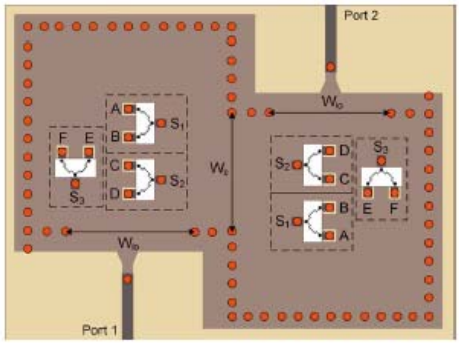

Fig. 25 Tunable SIW filter six tuning posts controlled by three SPDT RF MEMS switch packages[47]

The same switching principle was also proposed in [48] using PIN diodes. A fully tunable SIW filter is based on the mechanism of perturbing via posts located inside cavities. Appropriate positioning of these via posts provides both proper tuning and matching for various states. PIN diodes are selected to perform the switching task, and the proposed filter is fabricated on a three-layer PCB in order to separate the biasing circuit from the SIW filter.

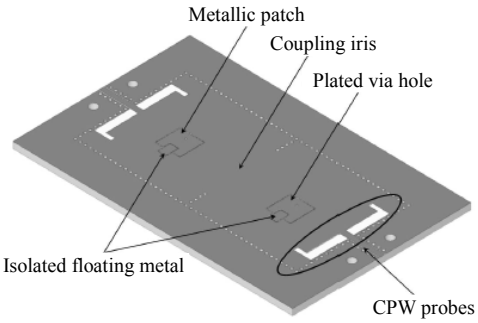

Fig. 26 Tunable SIW filter employing two varactor[49]

A tunable combline SIW resonator was proposed and studied in [49]. The capacitive loaded end of the resonator shown in Fig.26 has been used in order to include a surface-mounted tuning varactor diode that changes the resonant frequency of the device. The proposed device can be fabricated using a low-cost PCB process and using off-the-shelf GaAs varactor diodes. The structure presents a continuous tuning range of almost 20% with negligible power consumption.

Table 3 summarizes the performances of these reported tunable filters. The BST-based technique shows a better performance in term of bandwidth and insertion loss (IL). The insertion loss is more stable for the PIN diode type with a higher value. Probably, the lost energy is dissipated in the semiconductor devices and/or radiated.

Table 3 Comparison of various tunable filter performances

Type	Range/GHz	IL/dB	BW/(%)	Size/(λ_g^2)
BST[46]	2.95～3.57	3.3～2.2	5.4	0.47×0.35
MEMS[47]	1.2～1.6	2.2～4.1	3.7	1.3×1.3
PIN diode[48]	1.55～2	3.8～4.4	2.4～3	1.23×0.68
Varactor[49]	2.64～2.88	1.27～3.63	4	27×27.5

Very recently, a concept of two-dimensional tuning mechanism, which is based on the simultaneous use of both electric and magnetic tuning techniques has been proposed and demonstrated by the author's group[50]. The 2-D tuning is made possible thanks to the separable electric and magnetic fields within the SIW regions. This new technique allows the widening of tuning range and also it allows the simultaneous tuning of resonant frequency and inter-cavity coupling for dual-mode, cascaded or multi-cavity topology. This is critical to develop a frequency-agile tuning with constant bandwidth and frequency response over a wide frequency range.

3.2 Oscillators and VCOs

High-Q resonant cavities could be constructed with SIW technique. This has led to the development of novel SIW oscillators with low phase noise.

The topology of the proposed oscillator in [51] is illustrated in Fig. 27. It is a positive feedback circuit composed of an amplifier and SIW cavity that is formed on the same dielectric substrate. The SIW cavity acts as a frequency selector and at the same time as a coupling device for the positive feedback loop. The coupling level of the SIW cavity is adjusted so that the gain of the loop is slightly higher than 1 dB, to take into account the gain drop of the amplifier when it is in saturation. The loop length is also adjusted so to obtain 0 phase difference (Barkhausen stability criterion).

Low-phase-noise DRO (dielectric resonator oscillator) was discussed in [52], and an SIW circular cavity (SICC) is employed as the DR (dielectric resonator) to achieve higher quality factor instead of the rectangular type. It is composed of a hetero junction FET, an SICC structure resonator, a bias circuit and an SICC-to-microstrip transition. All of those are fabricated on the same dielectric substrate (Fig. 28). An SIW Gunn oscillator circuit proposed in [53] is illustrated in Fig. 29; it is composed of a Gunn diode and SIW resonant cavity, a direct current power supply circuit and a transition of SIW-to-microstrip. All of these components are integrated on the same dielectric substrate. The SIW cavity acts as resonator and at the same time as an energy-coupling device.

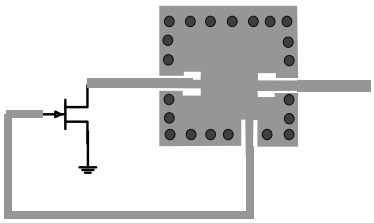

Fig. 27　Positive feedback oscillator

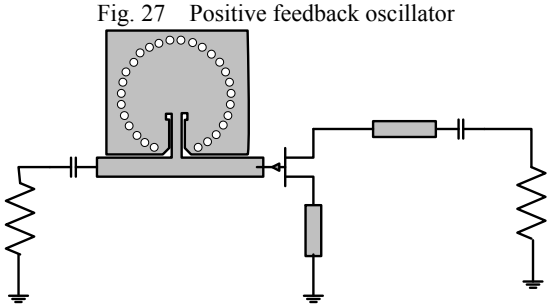

Fig. 28　DRO topology oscillator

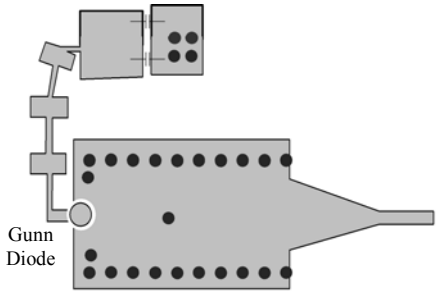

Fig. 29　Gunn diode oscillator

Table 4 compares performances of those mentioned different oscillators. The DRO shows a better phase noise thanks to the higher Q factor obtained by the SIW technique. The Gunn diode oscillator yields excellent results in terms of output power level with an excellent spectral purity.

The same principles of the positive and negative feedbacks were used to build VCO in [54-55], respectively. A comparison of reported continuously tunable SIW resonators and microwave SIW VCOs are listed in Tables 5 with tunable SIW cavity backed active antenna oscillator.

Table 4　Comparison of oscillator performances

Oscillator	Frequency/GHz	dBc/Hz	Power/dB
Positive feedback [51]	12.20	73@100KHz	0
DRO [52]	8.41	119 @10KHz	8.5
Gunn diode [53]	35.00	91@100KHz	15.2

Table 5　Comparison of SIW-enabled VCO performances

VCO	Frequency/GHz	BW/(%)	dBc/Hz
Positive feedback[54]	11.16～11.62	4.1	125
Negative feedback[55]	9.37～9.83	4.8	117
Tunable SIW antenna[56]	9.82～10.0	1.8	101

3.3　Amplifiers

SIW technique is known for its advantages such as high power handling capacity, low insertion loss, and low interference. Those advantages can be deployed for the purpose of harmonic suppression. In addition, the high-pass characteristics of SIW can be used for the separation of DC/low-frequency components and high-frequency signals. This is useful for high-frequency DC-biased circuit design such as RF and millimeter-wave amplifiers and other active components.

The first utilisation of SIW in amplifier design was related to a harmonics suppresser in [57-58]. Since the frequency of second harmonic components is lower than the inherent cut-off frequency of the SIW, the second harmonic components are blocked. At the same time, the third harmonic components are shorted by the shorted SIW. Measured results show that the second and third harmonic components can be reduced by 25 dB and 13 dB, respectively, compared to the outcomes using conventional high-impedance microstrip bias line. In [58], the proposed SIW-based harmonic suppression filter can suppress up to the 4^{th} harmonic with one single structure. The microstrip- based stub is connected with two SIW-based stubs. With measured results as shown in that work, the insertion loss of the proposed SIW based harmonic suppression filter at the 2^{nd}, 3^{rd}, and 4^{th} harmonics of 2.16 GHz is better than 33 dB, 15 dB, and 20 dB, respectively.

The second use is as input and output matching

networks as described in [59]. Each of these networks consists of a DC-decoupled transition and two iris-type inductive discontinuities. Since the inductive irises shown in Fig. 30 resemble short-circuited stubs, this configuration is similar to a double-stub matching network. Therefore, one can use the standard design procedure for this type of matching circuits. The DC-decoupled transition also serves as part of the matching structure. The presented X-band amplifier features a wideband uniform gain and appropriate return losses on its SIW ports over the entire frequency band of interest.

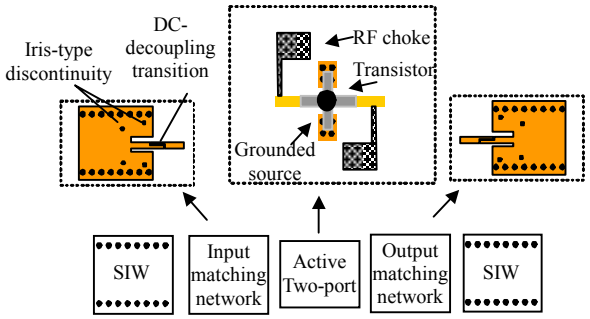

Fig. 30 Block diagram of the SIW Amplifier[59]

The third use of SIW as power divider/combiner is pertinent to the design of distributed amplifiers. Corrugated SIW (CSIW) makes use of open circuit quarter-wavelength stubs in place of vias to artificially create electric side-walls and isolate the top and bottom conductors at DC. Half-mode corrugated SIW (HMCSIW) was used, for example, in [60] to isolate the top and bottom walls from each other at DC. The HMCSIWs allow convenient biasing of the FETs without additional RF chokes and can be connected to HMSIWs via de-coupling capacitors. Distributed amplifier operating from 4 GHz ～ 7 GHz has demonstrated the feasibility of this approach.

3.4 Mixers

Sub-harmonic self-oscillating mixers (SOM) integrated with antenna were presented in [61-62]. An SOM circuit simultaneously provides both oscillating and mixing functions within a single block. Demonstrated at 30 GHz[61], this novel configuration makes use of SIW cavity as a resonator in the feedback loop to stabilize the fundamental oscillating frequency as illustrated in Fig. 31. This allows the possibility of building a complete planar receiver with improved phase noise. The circuit, implemented as a down-converter, exhibits an average conversion loss of 8.6dB, and an IF phase noise of −86 dBc/Hz at 100 kHz offset.

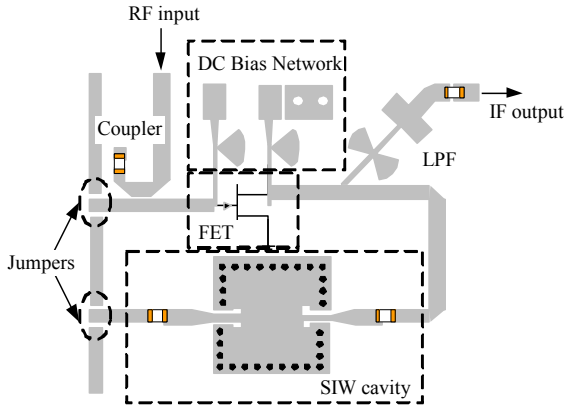

Fig. 31 Schematic diagram of the proposed SIW SOM[61]

Sub-harmonic up-converter has advantages in connection with the use of a lower frequency oscillator, which implies lower LO noise and adequate LO power level for the up-converter operation. However, spurious frequencies such as LO, 2LO, and images may reduce device performance. The cutoff frequency property of an SIW structure was effectively applied in [63] to suppress unwanted LO, 2LO and image components in the design of a sub-harmonic microwave up-converter. Experimental results show an additional 50 dB isolation is achieved with the SIW.

4 Antennas and Arrays

It is well recognized that the antenna is one of the most important system components that limit or enhance the system performance, depending the design of such a component. Generally, antenna elements cannot be conveniently integrated in chip-set because either they are too large or the required performance such as efficiency cannot be achieved by integrated components. In some cases, they could be simply considered as part of the package that embeds the chip-set, which may be of importance for millimeter-wave system design. In most high-gain antenna applications, array geometries are always required that involve both radiating elements and feed network. Special feed networks in the form of beam- forming networks present the engine for the development of multi-beam, beam-scanning and beam-agile systems.

4.1　Antenna elements

SIW supports the design of different antennas involving various elements and feeds as detailed in [8]. The more adaptable and popular antenna elements: slot (Fig. 32), patch backed by cavity (Fig. 33), and tapered slot antenna (Fig. 34) are presented in this section.

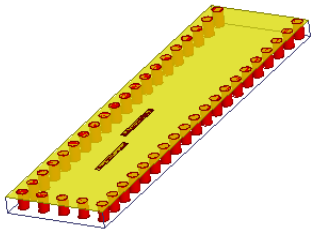

Fig. 32　Slot antenna

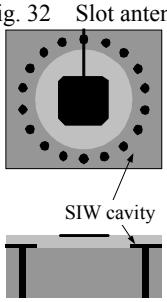

Fig. 33　Rectangular patch backed by circular cavity (Top and side view)

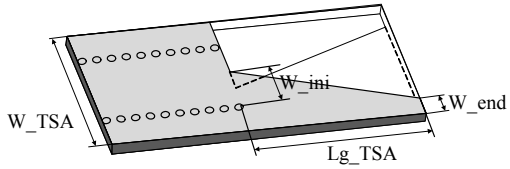

Fig. 34　Single-element configuration for the proposed SIW ALTSA

4.1.1　Slot antenna

As described in [64], the slots cut on the broad wall of the height-reduced dielectric-filled SIW along the longitudinal direction can be modeled approximately as shunt elements when the slot offset to the SIW center is small. Off-centered longitudinal slots, which disturb the transverse SIW surface currents, are spaced every half guided-wavelength to achieve a resonant element array when the mode is excited as shown in Fig. 32.

Compared to the standard waveguide, losses of SIW are higher since a dielectric substrate must be used to create this synthesized waveguide. However, the size reduction allows the implementation of more array elements, thus increasing the gain. A 32×32 array was developed at 94 GHz in [65]. To miniaturize the size of antennas, the technique of a half-mode SIW can be used in the design of slot array antennas[66]. One real advantage of SIW is the easiness of design and integration of the feeding network. A 12-way SIW power divider and 12 radiating SIWs each supporting 12 radiating slots were built in [67] for 60GHz applications (Fig. 35). Measured gain is about 22 dBi with a side lobe suppression of 25 dB in the H-plane and 15 dB in the E-plane while the bandwidth for 10 dB return loss is 2.5 GHz. Circularly-polarized traveling-wave antennas at 60 GHz using SIW technology were described in [68]. Elementary antenna building block composed of two inclined slots etched on the waveguide surface is characterized by full-wave simulations. High gain (more than 16 dB), excellent circular polarization and low side lobe level (up to –27dB) have been achieved.

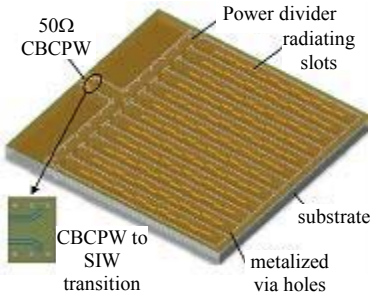

Fig. 35　SIW slot 12×12 array[67]

4.1.2　Patch antenna

The use of a thick substrate can increase the bandwidth of patch antenna but unfortunately cause the propagation of surface waves. These surface waves reduce the efficiency, increase cross-polarization radiation and limit the gain. To avoid these undesired effects, the patch antenna should be placed into a metallic cavity to suppress the surface waves, namely cavity-backed antennas. In a phased array antenna, cavities can prevent scan blindness, yield less coupling and improve good matching over a wider scan angle. The deployment of SIW technology would help in reducing the cost of realizing such cavity-backed antennas.

The proposed SIW cavity-backed patch antenna is comprised of a stack of two substrates as shown in Fig. 33. The cavities are emulated using vias, and the patches are driven by microstrip lines that are centrally fed by a shielded coaxial probe feed line. The measured 2×2 array performance in [69] exhibits an

aperture radiation efficiency of better than 70% over a wide frequency range from 11.5～12.71 GHz. With reference to one layer topology, design guidelines have been developed in [70], including via hole size and spacing, cavity shape and patch size. In [71], a 24 dBi of gain over 13% of bandwidth was achieved with an 8x8 array shown in Fig. 36.

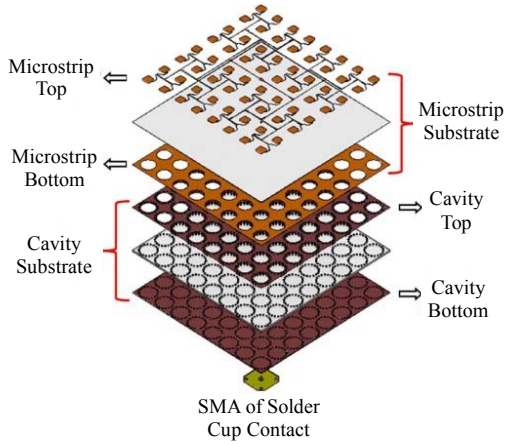

Fig. 36 SIW cavity-backed 8×8 patch antenna array[71]

4.1.3 Tapered slot antenna

An SIW-based tapered slot antenna (TSA) was demonstrated in which the metallization on either side of the substrate is flared in the opposite direction to form a tapered slot[72-73]. When SIW is used to feed the ALTSA (antipodal linearly tapered slot antenna), which is different from standard feed techniques, the bandwidth limitation caused by Balun can be removed and, thus wideband characteristics are indeed obtainable. Corrugations are well known in the design of horn antennas in which they are used to suppress higher modes. Therefore, they guarantee an excellent polarization pureness of antenna. Corrugated scheme was proposed in [74] for LTSA and in [75] for Fermi TSA. The cross-polarization level which is one of drawbacks of the standard TSA can be improved at excellent level. The beam width in the E-plane is generally large. With such a corrugation, this beam width becomes narrower, which it is very important in the design of a 2D array to generate a pencil beam. In [74], a 12-element linear array shows 19 dBi of gain and 19 dB for the SLL (side lobe level) with triangular amplitude taper. In [75], a 45 degree rotated E-to-H-plane interconnect ensures, with eight 1×16 and one 1×8 power dividers, the construction of one block feeding network for 128 antenna element array, as shown in Fig. 37. The gain of the planar array is 27 dBi, and the SLL is better than 26 dB in both E-plane and H-plane. The total weight of the entire array is less than 200 g, showing an important advantage of SIW technology in payload efficiency for space and airborne applications.

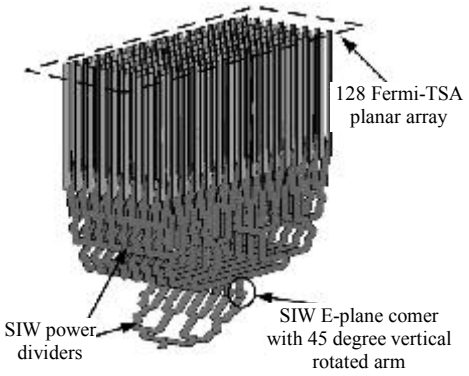

Fig. 37 Three-dimensional architecture of 128 element Fermi TSA antenna array[75]

4.2 Beamforming networks

Innovative and low-loss millimeter-wave antenna arrays and beamforming networks (BFN) based on SIW technology have been designed and developed for low-cost high-density integration and high-volume manufacturing. Different structures and architectures have been studied theoretically and experimentally. In the following, typical techniques and examples are shown for performances and features of various BFN structures.

4.2.1 Butler matrices

The Butler matrix is built by interconnecting couplers, phase shifters and crossovers. The crossovers increase the design complexity and path loss. Three Butler matrices are presented with three different topologies. The first of them, built at 77 GHz without crossover is shown in Fig. 38. This experimentally prototyped matrix is integrated with a four-array slot antenna on the same substrate[13]. An alternating offset is proposed to save the arrangement of input ports and to achieve broadband performances. For regular offset the simulated reflected power is below −10 dB from 75～79 GHz, which corresponds to 5.2% bandwidth. For the alternating offset array, the reflected power is below −10 dB from 72.5 GHz～81 GHz in simulation and measurement. The second structure is related to a

two-layer structure over 22～26 GHz frequency band. The double-layer structure illustrated in Fig. 39 is constructed using a combination of hybrids with broad-wall slot coupling[27]. The required phase shift is obtained by H-plane coupler inclinations. The change of layers occurs at places the second couplers stage and no crossing is required. To demonstrate the performance of the proposed matrix, the designed matrix is used to feed a four short ALTSA array. Subsequently, a 4×4 array antenna with longitudinal slots etched on the broad wall of SIW has been designed and integrated with the proposed matrix, which are then fabricated and measured. The proposed topology can easily be used to design 8×8 Butler matrices or higher.

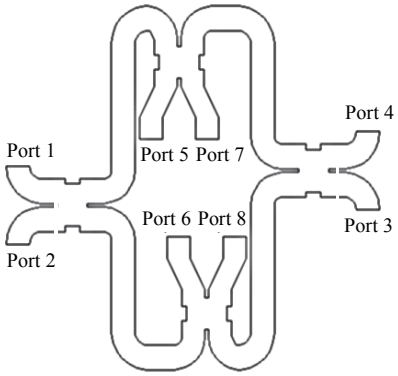

Fig. 38　SIW Butler matrix scheme without crossover

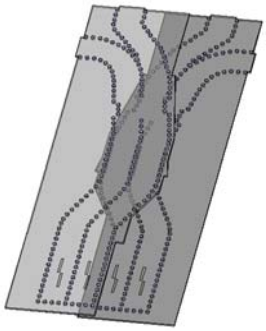

Fig. 39　Butler matrix scheme on a two-layer SIW structure

The third case is completely made planar with a cross-over at 12.5 GHz[76]. Wideband operation was achieved thanks to improved cross-couplers as shown in Fig. 40.

The use of SIW technology enables to reduce insertion losses compared to other printed technologies as shown in Table 6 while maintaining most advantages of such printed technologies such as high-density integration, manufacturing simplicity, and low weight compared to the waveguide counterparts. Good performances are confirmed over a 24% relative frequency bandwidth.

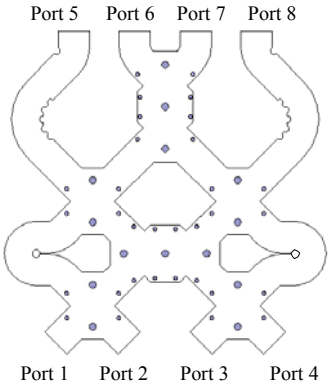

Fig. 40　Topology of planar SIW Butler matrix

Table 6　Comparison of Butler matrix performances

Technology	Configuration	Phase Error/(°)	Bandwidth /GHz	Loss /dB
SIW	Without crossing[13]	7	72～81	1.60
	Single layer[76]	±15	11～14	1.00
	Bi-layer[27]	±10	22～24	1.60
Waveguide	Bi-layer[77]	10	8.4～8.5	0.10
Microstrip	Single layer[78]	10	9～11	1.47
	Bi-layer[79]		5～6.5	4.00

4.2.2　Nolen and Blass Matrices

Blass matrices make use of transmission lines connected by power splitters and couplers to form multiple beam networks. When used as a BFN, the outputs of such matrices are linked to radiating elements and each input produces one beam. The phase delays required to produce the beam deviation for a given input are provided, adding extra transmission line lengths or phase shifters. Aperture amplitude distributions are controlled by the power splitter ratios.

A Ku-band double-layer 4×16 Blass matrix based on SIW technology was proposed in [80]. It is integrated with SIW slot antennas. A novel broad-wall-to- broad-wall slot coupler was used in the design. The altemating reverse-phase excitation was realized by reversing the offsets of the slots.

Two architectures of Nolen matrix were proposed and studied in [81]and in [18]. The first one is related to a perpendicular configuration in Ku band. The SIW cruciform couplers are used as fundamental building blocks for their wide range of coupling factors and specific topology well adapted to the serial feeding topology of a Nolen matrix (Fig. 41).

The frequency-dependent phase behavior of this matrix was expected, due to the serial feeding that

fundamentally characterizes a Blass or Nolen matrix. In fact, incremental phase shift between adjacent outputs varies with frequency. For instance, when the first input is used over the range f_0±0.25 GHz, the phase difference between adjacent outputs changes in turn by ±20 degree. And for a defined path array, the main beam scans from –5.3 degree～–15.3 degree. The second platform presents a parallel topology that shows a good performance over a broadband around 77 GHz. To achieve wide-band performances, the components of Nolen matrices are distributed in a more "parallel" topology, as shown in Fig 42. Parallel couplers are then preferred for this matrix design as they are more adapted to this new topology. The insertion phase of a direct port of coupler must be compensated for wide band operation.

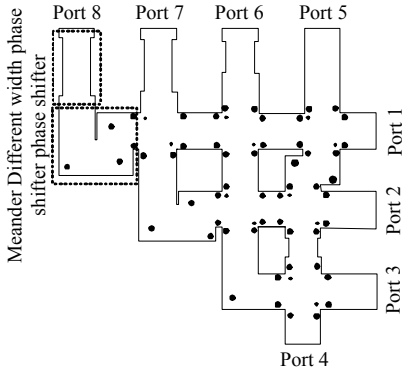

Fig. 41 Topology of standard SIW Nolen matrix configuration

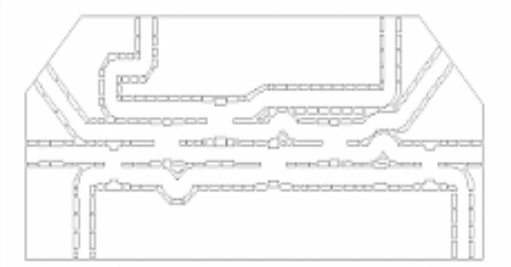

Fig. 42 Topology of modified SIW Nolen matrix configuration

The corresponding phase shifter is then added at different stage. The performances of these two SIW Nolen matrices with the Blass one are summarized in Table 7.

Table 7 Comparison of serial matrix performances

Matrix	Phase Error/(°)	Bandwidth /GHz	Loss /dB
Nolen Microstrip[82]	±18	2.15～2.25	0.9
Nolen SIW (1st design)[81]	±20	12.25～12.75	1.2
Nolen SIW (2nd design) [18]	±15	70～82	2.7
Blass SIW[80]	///	15.2～1.7	3.0
Blass Waveguide[83]	±10	11.32～11.82	1.2

4.2.3 Lens techniques

Fixed beams can also be formed using lens antennas such as Luneberg lens or Rotman lens with multiple feeds. Those structures are named in this way because of their ability to focus microwave or millimeter wave energy coming from a particular direction by passing the electromagnetic energy through a pair of parallel plates that are shaped like a lens.

In [84], we proposed a Rotman lens based on SIW technology. A similar design was described in [85]. The 7×9 SIW Rotman lens illustrated in Fig. 43 was developed with a corresponding multi-beam array antenna. The focal length was 28.6 mm and the beam directions were measured to be –41°, –28°, –14°, and 0 degree, and the gains were measured to be 13.8 dBi to 18.5 dBi, respectively, corresponding to input ports 1-4. This type of SIW Rotman lens is suitable to being conformal to a curved surface while preserving good characteristics.

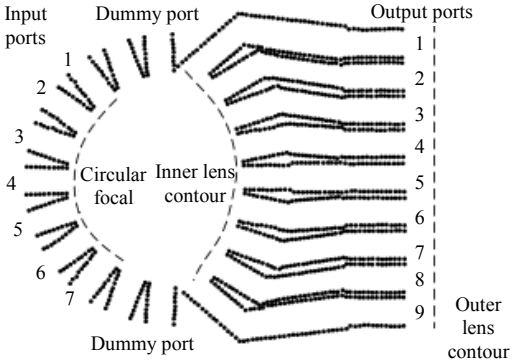

Fig. 43 Topology of SIW Nolen Rotman lens

In [86], a modified SIW R-KR lens was developed for linear array feeds, which operates at a center frequency of 30 GHz[16]. It had 15 input ports and 11 output ports, and the radius of the inner circle was 28 mm. Each output port is connected with an 8 elements slot-array antenna. This lens was able to cover a wide angle of (–59°, 59°) with its 3 dB beamwidth. The measured gains excited at different ports are ranged from 17.44 dBi～20.2 dBi while the radiation efficiencies were ranged from 21.6%～40.8%. A different reflector beam array was detailed in [87] and in [88]. In those two cases, leaky-wave beam steering characteristics combined with SIW BFN feeding are used to ensure 2-D scanning.

5 Future Outlooks and Remarks of SIW Technique

The above-discussed and reviewed active and passive components as well as antennas and arrays clearly show different advantages and features of the SIW technique used in various applications and scenarios. This review also suggests that the SIW component technologies based on PCB and other similar processes become matured and the next step will deal with the research and development of large-scaled system integration. Indeed, a number of front-ends in the format of system-on-substrate (SoS) has been demonstrated in the literature, which was not discussed in this article. For successfully deployments of SIW techniques, a full-scaled integration of various components on the same substrate will present the locomotive in the future research and development of RF and millimeter wave systems. This is particularly important for millimeter-wave and THz systems as the component-to-component integration cannot be made in hybrid-module or surface-mounting techniques. Monolithic integration based CMOS and MMIC processing platforms will be necessary in the future. Prior to doing so, this integration will be made at different level. As it becomes well-known, the SIW technique is definitely a promising candidate in the field of millimeter- and sub-millimeter-waves. However, the full potential of SIW and other integrated waveguide structures can only be exploited by combining them in hybrid SICs.

Different examples of SIW-based systems or subsystems have been demonstrated, which integrate different SIW parts with commercial active components such as the formation of a front-end at 24GHz in [89]; an FMCW radar in [90], a passive imaging system[91]. In [92], a fully-integrated 434 GHz transmitter in 0.13 μm SiGe BiCMOS was proposed including an on-chip SIW slot antenna. It has efficiency of 49.8% and antenna gain of –0.55 dBi.

The next generation of SICs will be built onto materials with different dielectric properties allowing the use of different transmission lines. Being synthesized on a planar substrate, substrate integrated image guide (SIIG) can be combined in a hybrid way with SIW as well as substrate integrated non-radiative dielectric guide (SINRD guide) on the same substrate. Of course, other non-planar structures such as rectangular coaxial lines can be synthesized into planar form. Therefore, SICs present a great flexibility and freedom in the choice and integration of different transmission line platforms. Those different planarized waveguides offer various guided-wave properties. In particular, some of the interested fundamental modes are orthogonal in space, which present extremely interesting solutions for creating small form-factor field-orthginal circuits and devices on the same planar substrate such as magic-T and orthogonal mode transducer (OMT). Of course, these guides will continue to get combined with the standard waveguide, microstrip, CPW or slotline, thereby constructing attractive hybrid schemes of planar and non-planar structures. High permittivity material can be used to build antenna feeding network in SINRD guide in order to reduce size and dielectric loss, and SIW can be used in filter and oscillator to benefit from the high Q with antenna integrated in low permittivity region of the proposed mixed waveguide plateform so as to increase the efficiency and density of integration.

A series of outlooks into future SICs-based developments have been envisaged in [93]. One of the most critical SICs developments in the future is related to active devices. Currently, all of active components are still limited to TEM modes, which are always voltage-and current-defined. At millimeter-wave and beyond, this will create significant problems because TEM-mode waveguide will be troubled by transmission loss, fabrication tolerance and other problems. Non-TEM modes offer much better solutions such as SIW, SIIG and SINRD guides. Therefore, the concept of “true” active waveguide techniques based on “nonlinear” media similar to the solid-state semiconductor devices should be developed. Such “active” waveguide should present “distributed” features with wave interactions instead of voltage- and current-characterized “lumped” elements that we have been working with since decades such as diodes and transistors. This will provide a truly disruptive

technology for millimeter-wave and THz systems, which should bridge the gap between electronics and photonics.

Of course, such active waveguides will provide "smart" and "performance-demanding" actions. Tunable waveguides can be realizable in the immediate future, which can perform distributed phase shifting that allows different modulation and smart antenna operation. To do so, innovative thick- and think-films and substrate such as ferroelectrics including BST, ferroelectric liquid crystal, VO_2, and electro-optical materials, can be integrated inside or as layer in SIW. It is also possible to develop active waveguide with traveling-wave Gunn diodes or three terminal devices based on the common line CPW/SIW techniques[94].

As the future of millimeter wave technology lies in successful hybrid integration techniques, it is therefore imperative to push forward and refine manufacturing and micro- and nano-fabrication processes in order to accommodate differing SICs structures on common platform for processing. With ever-increasing of operation frequency, it is very difficult to fabricate different components with required characteristics with the same processing techniques. The required machining accuracy, for example, is very difficult to satisfy because of sensitive dimensional tolerances. Conventional PCB-based fabrication process may fail to yield satisfactory precision in fabrication and alignment of SIW layouts at millimeter-wave frequencies (probably up to 100 GHz) as the design rule requires a certain degree of high-precision in the circuit geometry. Thus, a low-cost and high-precision technique is urgently required. The much-anticipated through-silicon-via (TSV) technology allows the 3-D integration of various SIW structures and SICs, which may present a natural technological platform for the design and realization of SICs[95]. With technological difficulties, the SICs are expected to be implemented within the framework of CMOS and MMICs for sub-millimeter-wave and THz applications as metallic or dielectric waveguides can be formed through those "standard" fabrication processes as long as appropriate design rules can be developed. This requires a substantial collaboration between academia and industry.

More recently, advances in the thick film technology have been made such as photoimageable and photoetchable conductor pastes, which have enabled system-in-package (SiP) techniques to be demonstrated well into the up-millimetre-wave frequency range up to 500 GHz[96]. LTCC technology has been known to well synergize with SIW techniques since it offers multilayered 3D passive integration. Our recently proposed LEGO-style blocks fabricated and assembled with easy-to-connect and manipulate PCB pieces have been proposed and demonstrated in [44] and [75]. This technique will play a critical role in the LTCC and PCB fabrication process.

Commercial applications require different components to work in different environmental conditions regarding temperature and moisture. In [97], it was demonstrated that with adequate selection of combined substrate properties, SIW cavities can provide self-temperature drift compensation. The compensation is achieved by using an appropriate ratio between the coefficient of thermal expansion and the thermal coefficient of the permittivity. The same concept was used successfully to stabilize the frequency of oscillation in [98]. The experiments also show that moisture absorption has more impact on microstrip filters. This is because SIW is an enclosed structure, which is less subject to moisture absorption. This is another advantage of SIW. Mechanical thermal fatigue has to be studied, which should show the limitation of different materials as SIW is presented as self-packaged structure.

There are numerous attempts in the use and development of SIW techniques for the design of RF, microwave and millimeter-wave systems.

Reference

[1] MEINEL H H. Commercial applications of millimeter waves-history, present status and future trends[J]. IEEE Transactions on Microwave Theory and Techniques, 1995, 44(7): 1639-1653.

[2] GOLDSMITH P F, HSIEH, C T, HUGUENIN G R, et al. Focal plane imaging systems for millimeter wavelengths[J]. IEEE Trans Microwave Theory and Techniques, 1993(41): 1664-1675.

[3] SALMON N A. Scene simulation for passive and active

millimetre and sub-millimetre wave imaging for security scanning and medical applications[J]. SPIE, 2004(5619): 129-135.

[4] ZHU L, WU K. Field-extracted lumped-element models of coplanar stripline circuits and discontinuities for accurate radio-frequency design and optimization[J]. IEEE Trans Microwave Theory and Tech, 2002, 50(4): 1207-1215.

[5] DESLANDES D, WU K. Accurate modeling, wave mechanisms, and design considerations of substrate integrated waveguide[J]. IEEE Trans Microwave Theory Tech, 2006(54): 2516-2526.

[6] BOZZI M, GEORGIADIS A. WU K. Review of substrate-integrated waveguide circuits and antennas[J]. IET Microwaves, Antennas & Propagation, 2011(5): 909-920.

[7] WU K. Integration and interconnect techniques of planar and nonplanar structures for microwave and millimeter-wave circuits-current status and future trend[C]//Asia–Pacific Microwave Conf. Taipei Taiwan china: [s.n.], 2001: 411-416.

[8] WU K, CHENG Y J, DJERAFI T, et al. Substrate integrated millimeter-wave and terahertz antenna technology[J]. IEEE Proceeding, 2012, 100(7): 2219-2232.

[9] WU K, DESLANDES D, CASSIVI Y. The substrate integrated circuits-a new concept for high-frequency electronics and optoelectronics[C]//6th International Conference on Telecommunications in Modern Satellite, Cable and Broadcasting Service. [S.l.]: [s.n.], 2003: P-III.

[10] VYE D. Divine innovation: 10 technologies changing the future of passive and control components[J]. Microwave Journal, 2011, 54(11): 22-42.

[11] DESLANDES D, WU K. Single-substrate integration technique of planar circuits and waveguide components[J]. IEEE Trans Microwave Theory Tech, 2003(51): 593-596.

[12] PATROVSKY A, DAIGLE M, WU K. Millimeter-wave wideband transition from CPW to substrate integrated waveguide on electrically thick high-permittivity substrates [C]//Proc 37th Eur Microw Conf Munich, Germany: [s.n.], 2007: 138-141.

[13] DJERAFI T, WU K. 77 GHz planar Butler matrix without crossover[J]. IEEE Transactions on Antennas and Propagation, 2012, 60(10): 4949-4954.

[14] CHEN X P, WU K. Systematic overview of substrate integrated waveguide (SIW) filters: design and performance tradeoffs[C]//Asia-Pacific Microwave Conference(APMC), workshop on Recent Progress in Filters and Couplers. Yokohama, Japan: [s.n.], 2010.

[15] WU K, CHEN X P. Concept of substrate integrated circuits applied to filter design and reachable performances [C]//European Microwave Week, WHM01 (EuMC) on recent advances in Substrate Integrated Waveguide Filters: Simulations, Technologies and Performances. Paris, France: [s.n.], 2010.

[16] CHENG Y J, WU K, HONG W. Power handling capability of substrate integrated waveguide interconnects and related transmission line systems[J]. Transactions on Advanced Packaging, 2008, 31(4): 900-909.

[17] CASSIVI Y, DESLANDES D, WU K. Substrate integrated waveguide directional couplers[C]//Proc Asia–Pacific Microw Conf. Kyoto, Japan: [s.n.], 2002: 1409-1412.

[18] DJERAFI T, FONSECA N. WU K. Broadband substrate integrated waveguide 4×4 Nolen matrix based on coupler delay compensation[J]. IEEE Trans Microw Theory Tech, 2011, 59(7): 1740-1745.

[19] HAO Z C, HONG W, CHEN J X, et al. Single-layer substrate integrated waveguide directional couplers[J]. Proc Inst Electr Eng, 2006, 153(5): 426-431.

[20] DJERAFI T. WU K. Super-compact substrate integrated waveguide cruciform directional coupler[J]. IEEE Microw Wireless Compon Lett, 2007, 17(11): 757-759.

[21] DJERAFI T, DAIGLE M, BOUTAYEB H, et al. Substrate integrated waveguide six-port broadband front-end circuit for millimeter-wave radio and radar systems[C]//Proc 39th EuMC. [S.l.]: [s.n.], 2009: 77-80.

[22] DJERAFI T, GAUTHIER J, WU K. Quasi-optical cruciform substrate integrated waveguide (SIW) coupler for millimeter-wave systems[C]//IEEE MTT-S Int Microwave Symposium Dig. Anaheim: [s.n.], 2010: 716-719.

[23] CHE W, DENG K, YUNG K N, et al. H-plane 3-db hybrid ring of high isolation in substrate integrated rectangular waveguide (SIRW)[J]. Microw Opt Techn Lett, 2006, 48(3): 502-505.

[24] DING Y, WU K. Miniaturized hybrid ring circuits using T-Type folded substrate integrated waveguide (TFSIW)[C]//IEEE Int Microw Symp, MTT-S. Boston: [s.n.], 2009: 705-708.

[25] DONG Y, ITOH T. Application of composite right/left-handed half-mode substrate integrated waveguide to the design of a dual-band rate-race coupler[C]//IEEE MTT-S Int Microwave Symposium Dig. Anaheim, CA, USA: [s.n.], 2010: 712-715.

[26] DJERAFI T, AUBERT H, WU K. Ridge substrate integrated waveguide (RSIW) dual-band hybrid ring coupler[J]. IEEE Microw Wireless Compon Lett, 2012, 22(2): 70-72.

[27] DJERAFI T, WU K. Multi-layered substrate integrated waveguide butler matrix for millimeter-wave systems[J]. International Journal of RF and Microwave Computer-Aided Engineering, 2012, 22(3): 336-344.

[28] DESLANDES D, WU K. Millimeter-wave substrate integrated waveguide filters[C]//IEEE Electrical Computer Engineering Canadian Conf. Canadian: [s.n.], 2003, 3(3): 1917-1920.

[29] HAO Z, HONG W, LI H, et al. A broadband substrate integrated waveguide (SIW) filter[C]//Proc IEEE Antennas Propag Soc Int Symp. [S.l.]:[s.n.], 2005, 1B: 598-601.

[30] MIRA F, BOZZI M. Efficient design of SIW filters by using equivalent circuit models and calibrated space-mapping optimization[J]. Int J RF Microwave Comput-Aided Eng, 2010, 20(6): 689-698.

[31] TANG H, HONG W, CHEN J, et al. Development of millimeter-wave planar diplexers based on complementary characters of dual-mode substrate integrated waveguide filters with circular and elliptic cavities[J]. IEEE Trans Microw Theory Tech, 2007, 55(4): 776-782.

[32] MIRA F, MATEU J, COGOLLOS S, et al. Design of ultrawideband substrate integrated waveguide (SIW) filters in zigzag topology[J]. IEEE Microwave Wireless Compon. Lett, 2009(19): 281-283.

[33] CHE W Q, LI C, DENG K, et al. Novel bandpass filter based on complementary split rings resonators and substrate integrated waveguide[J]. Microw Opt Technol Lett, 2008, 50(3): 699-701.

[34] FANG Z, HONG W, CHEN J X, et al. Cross-coupled substrate integrated waveguide filters with improved stopband performance[J]. IEEE Microwave and Wireless Components Letters, 2012, 22(12): 633-635.

[35] SHEN W, YIN W Y, SUN X W. Compact substrate integrated waveguide (SIW) filter with defect groud structure[J]. IEEE Microw Wirel Compon Lett, 2011, 21(2): 83-85.

[36] DOGHRI A, GHIOTTO A, DJERAFI T, et al. Compact and low cost substrate integrated waveguide cavity and bandpass filter using surface mount shorting stubs[C]// IEEE International Microwave Symposium Digest. Montreal, Qc, Canada: [s.n.], 2012: 1-3.

[37] HAO Z C, HONG W, CHEN X P, et al. Multilayered substrate integrated waveguide (MSIW) elliptic filter[J]. IEEE Microw Wireless Compon Lett, 2005, 15(2): 95-97.

[38] KRAMER O, DJERAFI T, WU, K. Dual-layered substrate integrated waveguide six-port with wideband double stub phase shifter[J]. IET Microwaves, Antennas & Propagation, 2012, 6(15): 1704-1709.

[39] BOUDREAU I, WU K, DESLANDES D, Broadband phase shifter using air holes in substrate integrated waveguide[C]//Microwave, MTT-S International Symposium-MTT. [S.l.]: [s.n.], 2011: 1-4.

[40] KIM K, BYUN J, LEE H Y. Substrate integrated waveguide wilkinson power divider with improved isolation performance[J]. Progress in Electromagnetics Research Letters, 2010(19): 41-48.

[41] DJERAFI T, HAMMOU D, TATU S, et al. Bi-layered substrate integrated waveguide wilkinson power divider/ combiner[C]//IEEE International Microwave Symposium Digest. Seattle: [s.n.], 2013: 1-3.

[42] D'ORAZIO W, WU K, HELSZAJN J. A substrate integrated waveguide degree-2 circulator[J]. IEEE Microwave Wireless Compon Lett, 2004(14): 207-209.

[43] D'ORAZIO W, WU K. Substrate integrated waveguide circulators suitable for millimeter-wave integration[J]. IEEE Trans Microwave Theory Tech, 2006(54): 3675-3680.

[44] YOUZKATLI E L, KHATIB B, DJERAFI T, et al. Substrate integrated waveguide vertical interconnects for three-dimensional integrated circuits[J]. Transactions on Components, Packaging and Manufacturing Technology, 2012, 2(9): 1526-1535.

[45] DJERAFI T, WU K. A 60 GHz substrate integrated waveguide crossover structure[C]//EUMC. Rome. Italy [s.n.], 2009: 1014-1017.

[46] ZHENG Y, SAZEGAR M, MAUNE H, et al. Compact substrate integrated waveguide tunable filter based on ferroelectric ceramics[J]. IEEE Microw Wireless Compon Lett, 2011, 21(9): 477-479.

[47] SEKAR V, ARMENDARIZ M, ENTESARI K. A 1.2-1.6 GHz substrate integrated- waveguide rf MEMS tunable filter[J]. IEEE Trans Microw Theory Techn, 2011, 59(4): 866-876.

[48] ARMENDARIZ M, SEKAR V, ENTESARI K. Tunable SIW bandpass filters with PIN diodes[C]//Proc 40th European Microwave Conference. Paris, France: [s.n.], 2010: 830-833.

[49] SIRCI S, MARTÍNEZ J D, TARONCHER M, et al. Low loss tunable filters in substrate integrated waveguide[J]. Waves, 2012(1): 70-78.

[50] ADHIKARI S, GHIOTTO A, WU K. Simultaneous electric and magnetic two-dimensionally tuned parameter-agile siw devices[J]. IEEE Trans on Microwave Theory and Technique, 2013(61): 423-435.

[51] CASSIVI Y, WU K. Low cost microwave oscillator using substrate integrated waveguide cavity[J]. IEEE Microw Wireless Compon Lett, 2003, 13(2): 48-50.

[52] QIANG L, YANG Y, HUANG K. Design of X-band oscillator based on substrate integrated circular cavity[C]// International Conference on Microwave and Millimeter Wave Technology (ICMMT). [S.l.]: [s.n.], 2012(1):1-3.

[53] ZHONG C L, XU J, YU Z Y, et al. X-band substrate integrated waveguide gunn oscillator[J]. IEEE Microw Wireless Compon Lett, 2008, 18(7): 461-463.

[54] CHEN Z, HONG W, CHEN J, et al. Design of high-Q tunable SIW resonator and its application to low phase noise VCO[J]. IEEE Microwave and Wireless Components Letters, 2013, 23(1): 43-45.

[55] HE F F, WU K, HONG W, et al. A low phase-noise VCO using an electronically tunable substrate integrated waveguide resonator[J]. IEEE Trans Microw Theory Tech, 2010, 58(12): 3452-3458.

[56] GIUPPI F, GEORGIADIS A, COLLADO A, et al. Tunable SIW cavity backed active antenna oscillator[J]. Electron Lett, 2010, 46(15): 1053-1055.

[57] HE F F, WU K, HONG W, et al. Suppression of second and third harmonics using lambda/4 low-impedance substrate integrated waveguide bias line in power amplifier[J]. IEEE Microwave Wireless Compon Lett, 2008(18): 479-481.

[58] WANG Z. PARK C W. Novel substrate integrated waveguide (SIW)-based power amplifier using siw-based filter to suppress up to the fourth harmonic[C]// Proceedings of APMC 2012. Kaohsiung, Taiwan, china: [s.n.], 2012: 830-832.

[59] MOSTAFA A, SHAHABADI M. X-band substrate

integrated waveguide amplifier[J]. Microwave and Wireless Components Letters, 2008, 18(12): 815-817.
[60] ECCLESTON K W. Corrugated substrate integrated waveguide distributed amplifier[C]//In Microwave Conference Proceedings (APMC). [S.l.]: [s.n.], 2012: 379-381.
[61] JIJUN X, WU K. A subharmonic self-oscillating mixer using substrate integrated waveguide cavity for millimeter-wave application[C]//IEEE MTT-S International Microwave Symposium Digest. [S.l.]: [s.n.], 2005: 1-4.
[62] ZHANG Z Y, WU K, YANG N. A millimeter-wave sub-harmonic self-oscillating mixer using dual-mode substrate integrated waveguide cavity[J]. IEEE Transactions on Microwave Theory and Techniques, 2010, 58(5): 1151-1158.
[63] CHEN J X, HONG W, HAO Z C, et al. High isolation sub-harmonic up-converter using substrate integrated waveguide[J]. Electron Lett, 2005, 41(22): 1225 -1226.
[64] YAN L, HONG W, HUA G, et al. Simulation and experiment on SIW slot array antennas[J]. IEEE Microwave and Wireless Components Letters, 2004, 14(9): 446-448.
[65] CHENG Y J, HONG W, FAN Y, et al. 94 GHz substrate integrated monopulse antenna array[J]. IEEE Trans Antennas Propag, 2012, 60(1): 1-9.
[66] CHENG Y J, HONG W, WU K. Millimeter-wave half mode substrate integrated waveguide frequency scanning antenna with quadri-polarization[J]. IEEE Trans Antennas Propag, 2010, 58(6): 1848-1855.
[67] CHEN X P, WU K, HAN L, et al. Low-cost high gain planar antenna array for 60-ghz band applications[J]. IEEE Transactions on Antennas and Propagation, 2010, 58(6): 2126-2129.
[68] NEMATOLLAHI H, BOUTAYEB H, WU K. Millimeter-wave circularly-polarized traveling-wave substrate integrated waveguide antennas[C]//In Microwave Conference. [S.l.]: [s.n.], 2009: 1555-1558.
[69] AWIDA M H, FATHY A E. Substrate integrated waveguide ku-band cavity-backed 2×2 microstrip patch array antenna [J]. IEEE Antennas Wirel Propag Lett, 2008(8): 1054-1056.
[70] AWIDA M H, FATHY A. E. Design guidelines of substrate-integrated cavity backed patch antennas[J]. IET Microwaves, Antennas & Propagation, 2012, 6(2): 151-157.
[71] AWIDA M H, SULEIMAN S H, FATHY A E. Substrate-integrated cavity-backed patch arrays: a low-cost approach for bandwidth enhancement[J]. IEEE Trans Antennas Propag, 2011, 59(4): 1155-1163.
[72] HAO Z C, HONG W, CHEN J X, et al. Novel feeding technique for antipodal linearly tapered slot antenna array[C]//IEEE IMS 2005. Long Beach, California, USA: [s.n.], 2005: 1641-1644.
[73] CHEN Y J, HONG W, WU K. Design of a monopulse antenna using a dual v-type linearly tapered slot antenna[J]. IEEE trans on Ant and Prop, 2008, 56(9): 2903-2909.
[74] DJERAFI T, WU K. Corrugated substrate integrated waveguide (SIW) antipodal linearly tapered slot antenna array fed by quasi-triangular power divider[J]. Progress In Electromagnetics Research C, 2012(26): 139-151.
[75] YOUZKATLI E L, KHATIB B, DJERAFI T, et al. Three-dimensional architecture of substrate integrated waveguide feeder for fermi tapered slot antenna array applications[J]. IEEE Transactions on Antennas and Propagation, 2012, 60(10): 4610-4618.
[76] DJERAFI T, FONSECA N J G, WU K. Design and implementation of a planar 4×4 Butler matrix in SIW technology for wide band high power applications[J]. Progress In Electromagnetics Research B, 2011(35): 29-51.
[77] HIROKAWA J, FURUKAWA M, TSUNEKAWA K, et al. Double-layer structure of rectangular-waveguides for Butler matrix[C]//32nd European Microwave Conf. [S.l.]: [s.n.], 2002: 1-4.
[78] HE J, WANG B Z, HE Q Q, et al. Wideband X-band microstrip Butler matrix[J]. Progress In Electromagnetics Research, 2007(74): 131-140.
[79] TRAII M, NEDIL M, GHARSALLAH A, et al. A novel wideband butler matrix using multi-layer technology[J]. Microwave and optical technology letters, 2009, 51(3): 659-663.
[80] CHEN P, HONG W, KUAI Z Q, et al. A double layer substrate integrated waveguide Blass matrix for beamforming applications[J]. IEEE Microwave and Wireless Components Letters, 2009, 19(6): 374-376.
[81] DJERAFI T, FONSECA N J G, WU K. Planar Ku-band 4x4 Nolen matrix in SIW technology[J]. IEEE Transactions on Microwave Theory and Techniques, 2011, 58(2): 259-266.
[82] FONSECA N J G. Printed S-band 4×4 Nolen matrix for multiple beam antenna applications[J]. IEEE Trans Antennas Propag, 2009, 57(6): 1673-1678.
[83] CASINI F, GATTI R, VMARCACCIOLI L, et al. A novel design method for Blass matrix beam-forming networks [C]//Proc Eur Microw Conf. [S.l.]: [s.n.], 2007: 1511-1514.
[84] CHENG Y, HONG W, WU K, et al. Substrate integrated waveguide (SIW) rotman lens and its Ka-band multibeam array antenna applications[J]. IEEE Transactions on Antennas and Propagation, 2008, 56(8): 2504-2513.
[85] SBARRA E, MARCACCIOLI L, GATTI R V, et al. A novel Rotman lens in SIW technology[C]//37th European Microwave Conference. [S.l.] : [s.n.], 2007: 1515-1518.
[86] CHENG Y L, HONG W, WU K. Design of a substrate integrated waveguide modified R-KR lens for millimetrewave application[J]. IET Microwaves, Antennas and Propagation, 2010, 4(4): 484-491.
[87] ETTORRE M, SAULEAU R, LE COQ A. Multi-Beam multi-layer leaky-wave SIW pillbox antenna for millimeter-wave applications[J]. IEEE Transactions on Antennas and Propagation, 2011, 59(4): 1093-1100.
[88] CHENG Y J, HONG W, WU K, et al. Millimeter-wave substrate integrated waveguide long slot leaky-wave

antennas and two-dimensional multibeam applications[J]. IEEE Transactions on Antennas and Propagation, 2011, 59(1): 4047.

[89] ZHANG Z Y, WEI Y R, WU K. Broadband millimeter-wave single balanced mixer and its applications to substrate integrated wireless systems[J]. IEEE Transactions on Microwave Theory and Techniques, 2012, 60(3): 660-669.

[90] ZHAOLONG L, WU K. 24-GHz frequency-modulation continuous-wave radar front-end system-on-substrate[J]. IEEE Transactions on Microwave Theory and Techniques, 2008, 56(2): 278-285.

[91] DOGHRI A, DJERAFI T, GHEOTO A, et al. Broadband substrate-integrated-waveguide six-port applied to the development of polarimetric imaging radiometer[C]// EUMC. Manchester: [s.n.], 2011: 393-396.

[92] HU S, WANG L, XIONG Y Z, et al. A 434 GHz SiGe BiCMOS transmitter with an on-chip SIW slot antenna[C]// IEEE Asian Solid-State Circuits Conference. [S.l.] : [s.n.], 2011: 269-273.

[93] WU K. Substrate integrated circuits (SICs) for terahertz electronics and photonics: current status and future outlook[J]. FREQUENZ, 2011(65): 255-259.

[94] PATROVSKY A, DAIGLE M, WU K. Coupling mechanism in hybrid SIW-CPW forward couplers for millimeter wave substrate integrated circuits[J]. IEEE Trans Microwave Theory Tech, 2008, 56(11): 2594-2601.

[95] HU S M, WANG L, XIONG Y Z, et al. TSV technology for millimeter-wave and terahertz design and applications[J]. IEEE Trans Compon, Packag Manufacturing Tech, 2011, 1(2): 260-267.

[96] STEPHENS D, YOUNG R, ROBERTSON I D. Millimeter-wave substrate integrated waveguides and filters in photoimageable thick-film technology[J]. IEEE Trans Microw Theory Tech, 2005, 53(12): 3832-3838.

[97] DJERAFI T, DESLANDES D, WU K. A temperature compensation technique for substrate integrated waveguide cavities and filters[J]. IEEE Transactions on Microwave Theory and Techniques, 2012, 60(8): 2448-2455.

[98] DJERAFI T, DESLANDES D, WU K. Temperature drift compensation technique for substrate integrated waveguide oscillator[J]. IEEE Microwave and Wireless Components Letters, 2012, 2(9): 489-491.

编 辑 蒋 晓